© MAY 2023 | IRE Journals | Volume 6 Issue 11 | ISSN: 2456-8880
DOI: https://doi.org/10.64388/IREV6I11-1722650

Low-Velocity Impact Response and Force Transmission in 2D Architected Sandwich Cores: Effect of Cell Angle and Functional Grading

BAMIDELE FADAYOMI
Department of Mechanical Engineering, Texas A&M University

Abstract-* *Architected sandwich cores intended for protective applications must be assessed on the force they transmit to a protected substrate, not only on the load they withstand. This study reports the low-velocity impact response of eight two-dimensional architected sandwich core configurations and evaluates them on transmitted force and damage containment. Honeycomb cores at unit-cell angles of 15°, 30° and 45°, diamond cores at 45°, 90° and 120°, and a functionally graded variant of each topology were additively manufactured from a UV-cured brittle photopolymer and each subjected to a single low-velocity impact from an 18 N steel sphere released from 300 mm, corresponding to a nominal incident energy of 5.4 J, with five replicate specimens per configuration. Transmitted force was recorded at a sensor beneath the panel and the fracture process was captured by high-speed imaging. Peak transmitted force varied by a factor of 3.2 across the configuration set, from 2447.08 ± 42.38 N for the 45° diamond core to 761.02 ± 27.30 N for the 120° diamond core. The two topologies behaved differently: all honeycomb configurations transmitted between 1698 and 1946 N and were insensitive to cell angle, whereas the diamond configurations spanned the full range and were strongly angle-dependent. The configurations transmitting the lowest force also fractured least, dissipating incident energy through large-scale compliant core deformation rather than through cracking, and exhibited correspondingly broader force-time profiles. Comparison against quasi-static data for the same configurations shows that the stiffness ranking established under static loading is preserved under impact, consistent with the Type I and Type II framework, but that the ranking by protective performance is inverted: the stiffest configuration is the poorest attenuator. Functional grading additionally confined damage to prescribed core regions while leaving stiffer regions intact. These results indicate that cell angle in the diamond topology functions as a single geometric parameter selecting between structural and protective performance regimes.

Keywords: architected materials; sandwich structures; low-velocity impact; force transmission; energy absorption; functionally graded lattices; high-speed imaging; additive manufacturing

I. INTRODUCTION

Sandwich panels with architected cores are used in aerospace, naval, automotive and protective structures because they combine low areal mass with high bending stiffness [1,2]. In many of these applications the governing load case is not quasi-static but transient: tool drop, hail, runway debris, minor collision and handling damage all impose localised low-velocity impact. Such events are significant precisely because they can produce internal core damage while leaving the outer face sheet visually intact, degrading residual capacity without obvious external indication [4,5].

Most characterisation of architected cores under impact is framed in terms of absorbed energy and peak sustained load. For a panel whose purpose is to protect something behind it, however, the more directly relevant quantity is the force transmitted through the panel to the protected substrate. A core that fractures early and extensively may absorb considerable energy while still transmitting a high peak force; conversely a compliant core may transmit little force by deforming over a longer interval. These are distinct performance measures and they do not necessarily rank architectures in the same order. Transmitted force is comparatively seldom reported for parametric sets of architected cores, and it is the primary measurement in the present study.

A second open question concerns the transferability of quasi-static characterisation to dynamic loading. Calladine and English [3] distinguished Type I structures, which exhibit a flat or rising load-deflection response, from Type II structures, which exhibit a sharp initial peak followed by softening, and argued that the two classes respond differently to rate and inertia effects, with Type II structures being the more rate-sensitive. Their framework implies that a structure retains its characteristic response class under impact provided the impact velocity is insufficient to alter the quasi-static collapse mode. Whether that expectation holds for additively manufactured brittle architected cores, whose collapse involves fracture rather than plastic hinging, is not established.

Prior work has examined impact in printed lattice-cored sandwich panels, including auxetic and non-auxetic cores [6] and multi-hit meta-sandwich configurations [5], and has shown that graded lattices can improve energy absorption relative to uniform ones [7,8]. What remains less well characterised is how a single geometric parameter, systematically varied across two topologies with all other variables fixed, governs the transition between structural and protective behaviour under impact.

This study addresses that question. Eight core configurations spanning two topologies, three cell angles each and a functionally graded variant of each, were subjected to identical low-velocity impact with five replicates per configuration. The specific objectives were: (i) to quantify peak transmitted force as a function of topology, cell angle and grading; (ii) to relate transmitted force to the observed damage mechanism, distinguishing energy dissipation by fracture from dissipation by core deformation; and (iii) to determine whether the response classification established under quasi-static loading is preserved under impact. Quasi-static failure behaviour of the same configurations is reported separately in a companion study [9]; the present paper is concerned with dynamic response and with the static-to-dynamic comparison.

II. MATERIALS AND METHODS

2.1 Core architectures

Two planar core topologies were examined. The honeycomb core consists of tessellated hexagonal unit cells in an in-plane orientation; the diamond core is a reoriented square lattice. A single characteristic unit-cell angle θ was varied parametrically within each topology while wall thickness and core envelope were held fixed: 15°, 30° and 45° for honeycomb, and 45°, 90° and 120° for diamond. The angular ranges differ because the two topologies become geometrically degenerate at different angles.

A functionally graded variant of each topology was also produced, in which vertical cell height was graded through the core thickness according to a prescribed growth function. This creates a monotonic through-thickness compliance gradient without altering the in-plane topology. Eight configurations resulted: four honeycomb and four diamond.

2.2 Specimen geometry, material and manufacturing

Impact specimens were sandwich panels measuring 80 x 80 x 48 mm, with face plate thickness fixed at 4 mm and core thickness at 40 mm across all configurations. Geometry was modelled in SOLIDWORKS 2021, except the functionally graded honeycomb, which was constructed in Blender v3.3.1 to implement the grading function directly.

All panels were manufactured from ANYCUBIC Basic UV-curable photopolymer resin, comprising approximately 60 percent epoxy resins, 35 percent (1-methyl-1,2-ethanediyl)bis[oxy(methyl-2,1-ethanediyl)] diacrylate and 5 percent hydroxycyclohexyl phenyl ketone. A brittle post-cure constituent was selected so that fracture would be directly observable rather than masked by distributed plastic deformation. Panels were printed on an ANYCUBIC Photon Mono X LCD resin printer, washed in 99 percent isopropyl alcohol for 5 to 10 minutes, post-cured for 2 minutes in an ANYCUBIC UV curing station, and oriented at 45° during printing to limit warping. Forty panels were tested under impact, comprising five replicates of each of the eight configurations.

Constituent properties were characterised separately to ASTM D638-14, C1161-13 and D695-15. The cured resin exhibited a tensile strength of 22.192 ± 2.317 MPa, tensile modulus of 0.528 ± 0.040 GPa, flexural strength of 25.193 ± 2.240 MPa, flexural stiffness of 0.608 ± 0.074 GPa, compressive strength of 55.785 ± 6.474 MPa and compressive stiffness of 1.048 ± 0.069 GPa, failing abruptly at peak stress with negligible post-peak ductility.

2.3 Low-velocity impact procedure

Impact was applied by releasing a 76.2 mm (3 inch) diameter steel ball bearing of 18 N weight,

© MAY 2023 | IRE Journals | Volume 6 Issue 11 | ISSN: 2456-8880
DOI: https://doi.org/10.64388/IREV6I11-1722650

corresponding to a mass of approximately 1.835 kg, from a height of 300 mm through a 76.2 mm guide tube onto the centre of the panel (Figure 1). Each panel received a single impact. Neglecting friction and aerodynamic drag within the guide tube, this corresponds to a nominal impact velocity of 2.43 m/s and a nominal incident energy of 5.4 J.

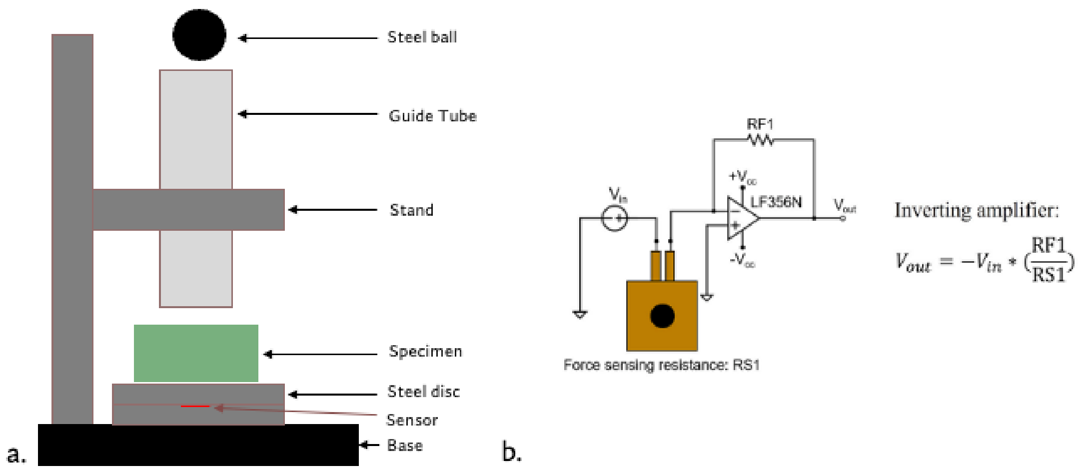

Figure 1. a) Low-velocity impact test setup, showing the steel ball, guide tube, specimen, steel disc and pressure sensor; b) inverting-amplifier circuit for the pressure sensor.

The panel was seated on a circular disc positioned above a pressure sensor. Sensor output was acquired through an inverting amplifier with a 10 kilohm resistor by a National Instruments myDAQ data acquisition system operated through LabVIEW. The fracture process was recorded by a Phantom v5.2 high-speed camera. All tests were conducted at room temperature with five replicates per configuration.

An important measurement convention applies throughout. The recorded quantity is the force transmitted through the panel to the sensor beneath it, not the contact force at the impact point on the upper face. This is the appropriate measure for assessing protective performance, since it represents what a protected substrate would experience, but it means that reported peak forces should not be interpreted as impactor contact forces. A configuration recording a low peak transmitted force is attenuating the event, not sustaining a lower load.

III. RESULTS

3.1 Peak transmitted force

Peak transmitted force varied by a factor of 3.2 across the eight configurations, from 2447.08 ± 42.38 N to 761.02 ± 27.30 N. The two topologies divided sharply in their sensitivity to cell angle. All four honeycomb configurations transmitted between 1698.62 ± 200.29 N and 1945.27 ± 43.44 N, a spread of only about 15 percent, indicating that cell angle exerts little influence on force transmission in this topology. Within that narrow band, transmitted force increased modestly and monotonically with θ, from 1698.62 N at 15° to 1926.47 ± 68.17 N at 45°, with the functionally graded honeycomb highest at 1945.27 N.

The diamond configurations spanned the entire range. The 45° diamond core transmitted the highest force of any configuration, 2447.08 ± 42.38 N, with the lowest relative scatter observed in the study at 1.7 percent of the mean (Figure 2). Increasing θ to 90° reduced transmitted force to 1736.73 ± 295.31 N, and at 120° it fell to 761.02 ± 27.30 N, a reduction of 69 percent relative to the 45° configuration. The functionally graded diamond core transmitted 775.35 ± 102.59 N, comparable to the 120° configuration. Results are summarised in Table 1.

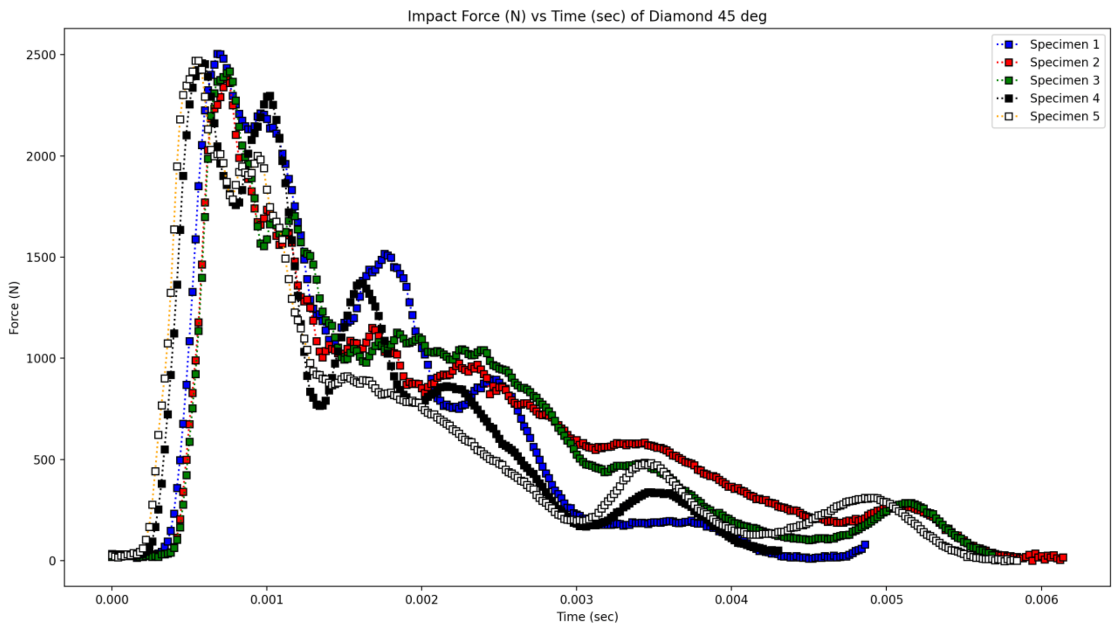

Figure 2. Transmitted force versus time for the five 45° diamond sandwich panels, showing peak loads exceeding 2400 N with close repeatability across replicates.

Table 1. Peak transmitted force, coefficient of variation and damage extent under a single low-velocity impact at 5.4 J nominal incident energy (mean ± standard deviation, five replicates per configuration).

Configuration	Peak transmitted force (N)	CV (%)	Damage extent
Honeycomb 15°	1698.62 ± 200.29	11.8	Rows 1–2
Honeycomb 30°	1741.61 ± 187.32	10.8	Rows 1–2
Honeycomb 45°	1926.47 ± 68.17	3.5	Propagates to bottom corner
Honeycomb graded	1945.27 ± 43.44	2.2	Confined to centre
Diamond 45°	2447.08 ± 42.38	1.7	Row 1 only; no deflection
Diamond 90°	1736.73 ± 295.31	17.0	Rows 1–2
Diamond 120°	761.02 ± 27.30	3.6	Minimal fracture; large deformation
Diamond graded	775.35 ± 102.59	13.2	Rows 1–2, face sheet and upper edges

© MAY 2023 | IRE Journals | Volume 6 Issue 11 | ISSN: 2456-8880
DOI: https://doi.org/10.64388/IREV6I11-1722650

3.2 Damage mechanisms

Damage extent correlated inversely with transmitted force. The 45° diamond core, which transmitted the highest force, sustained the least damage: fracture was confined to the first row at the direct impact point and did not propagate to the front plane, and face sheet deflection was negligible (Figure 3). This configuration behaves as a stiff transmission path, passing the impulse to the substrate substantially undiminished rather than dissipating it internally.

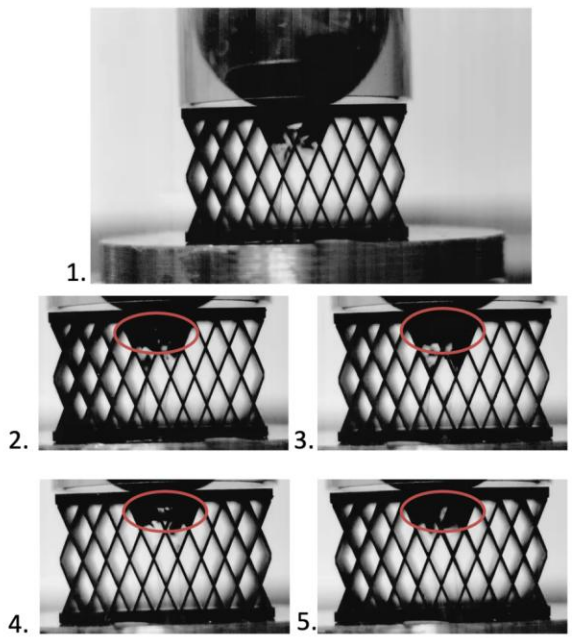

Figure 3. Post-impact condition of the five 45° diamond sandwich panels. Fracture is confined to the first row at the impact point, with negligible face sheet deflection.

At the opposite extreme, the 120° diamond core, which transmitted the lowest force, showed little to no fracture in four of five replicates but underwent extensive face sheet and core deformation (Figure 5). Energy was dissipated through large-scale compliant deformation of the core rather than through crack formation. The functionally graded diamond core transmitted a comparable force but sustained more fracture than the 120° configuration, concentrated in the face sheet and upper row edges, while the stiffer lower rows resisted deformation.

The honeycomb configurations occupied an intermediate regime, with fracture generally confined to the first and second rows. Two exceptions are notable. In the 45° honeycomb, damage propagated beyond the impact region toward the bottom corner of the panel, indicating a crack path not arrested by the surrounding cell structure. In the functionally graded honeycomb, damage was confined within the central region, and face sheet deflection was less pronounced than in the 15° and 30° configurations.

3.3 Force-time response

Force-time profiles differed systematically between the high-transmission and low-transmission configurations. The 45° diamond core produced a sharp, high-amplitude impulse with a well-defined peak exceeding 2400 N and a broad plateau reflecting subsequent core dissipation, reproduced closely across all five replicates (Figure 2). The 120° diamond core produced a substantially lower peak of approximately 760 N distributed over a visibly broader time interval (Figure 4).

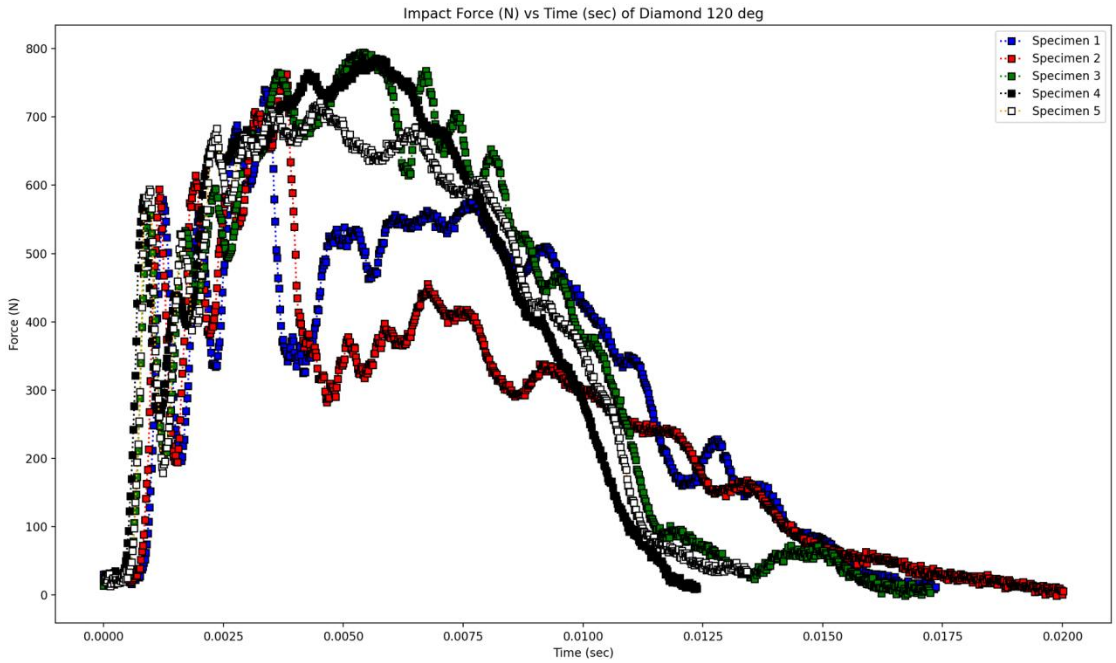

Figure 4. Transmitted force versus time for the five 120° diamond sandwich panels, showing substantially lower peak forces distributed over a broader interval than the 45° configuration in Figure 2.

This broadening is the mechanical signature of the attenuation reported in Section 3.1. For a fixed incident momentum, extending the duration over which the impulse is delivered necessarily reduces its peak amplitude. The compliant core lengthens the contact event and thereby limits the instantaneous force reaching the substrate, whereas the stiff core delivers the same impulse over a shorter interval at higher amplitude.

© MAY 2023 | IRE Journals | Volume 6 Issue 11 | ISSN: 2456-8880
DOI: https://doi.org/10.64388/IREV6I11-1722650

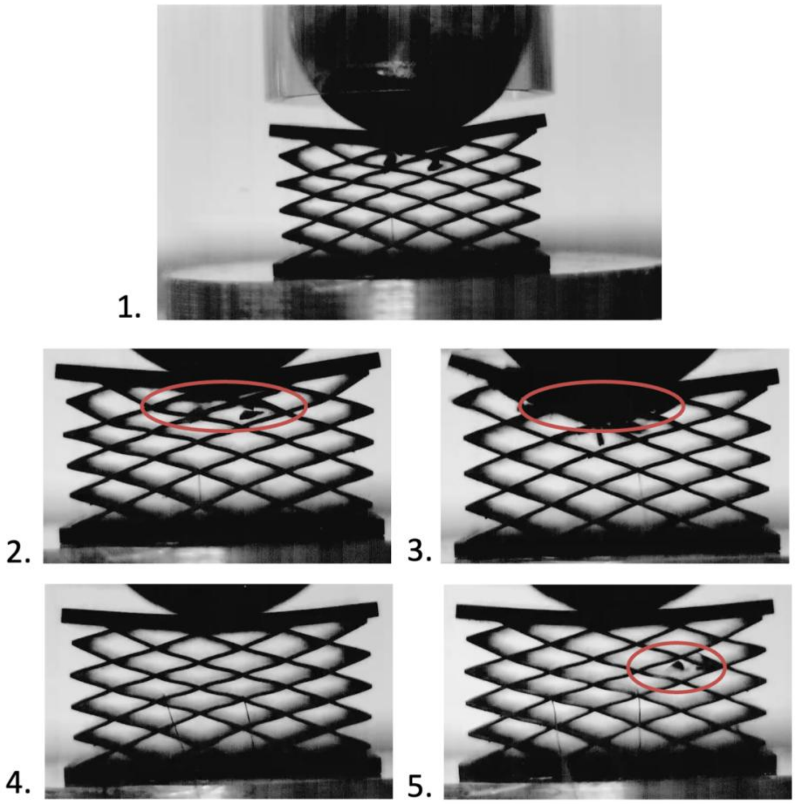

Figure 5. Post-impact condition of the five 120° diamond sandwich panels: little to no core fracture, with impact energy dissipated through large-scale core and face sheet deformation.

3.4 Response reproducibility

The shape of the force-time response was markedly less consistent under impact than the corresponding load-displacement response of the same configurations under quasi-static loading, particularly for the honeycomb family, and no recurring load-time pattern emerged within the honeycomb categories. The magnitude of the peak transmitted force was nonetheless repeatable, with coefficients of variation ranging from 1.7 percent for the 45° diamond core to 17.0 percent for the 90° diamond core, a range comparable to that observed quasi-statically. The distinction matters for model validation: peak transmitted force is a stable validation target across all configurations, whereas the full force-time history is a meaningful target only for the configurations at the extremes of the stiffness range.

The configurations at the two extremes of transmitted force were the most repeatable, with coefficients of variation of 1.7 percent for the 45° diamond and 3.6 percent for the 120° diamond. The intermediate configurations were the most variable. A plausible interpretation is that the extreme configurations are governed by a single dominant mechanism, stiff transmission in the first case and compliant deformation in the second, whereas the intermediate configurations involve competition between fracture and deformation whose balance is sensitive to the precise position of the impact point relative to the underlying strut array.

IV. DISCUSSION

4.1 Cell angle selects between structural and protective regimes

The central result is that in the diamond topology a single geometric parameter selects between two qualitatively different performance regimes. At 45° the core is a stiff structural element: it resists local damage, confining fracture to the first row, but transmits 2447 N to the substrate. At 120° the same

© MAY 2023 | IRE Journals | Volume 6 Issue 11 | ISSN: 2456-8880
DOI: https://doi.org/10.64388/IREV6I11-1722650

topology becomes a protective element: it transmits only 761 N, a 69 percent reduction, at the cost of large core deformation.

These are not two points on a single performance scale but two distinct dissipation strategies. The stiff configuration preserves its own integrity and passes the event through; the compliant configuration sacrifices its geometry to attenuate the event. Which is preferable depends entirely on what the panel is required to do. Where the panel is itself the load-bearing structure and must survive impact with minimal damage, the 45° configuration is appropriate. Where the panel protects something behind it, the 120° configuration is appropriate, and the stiffest architecture is in fact the worst available choice.

The honeycomb topology does not offer this selectivity. Transmitted force varied by only about 15 percent across its full angular range, so cell angle in the honeycomb cores is not an effective design lever for impact attenuation. This asymmetry between the topologies mirrors their behaviour under quasi-static loading [9], where the diamond family also spanned a far wider performance range than the honeycomb family.

4.2 Static ranking is preserved, protective ranking is inverted

Comparison with quasi-static data for the same configurations [9], summarised in Table 2, shows that the stiffness ordering established statically carries over to impact. The 45° diamond core recorded both the highest quasi-static compressive peak load, at 8455.89 N, and the highest transmitted impact force, at 2447.08 N. The 120° diamond core recorded the lowest of each, at 408.19 N and 761.02 N respectively. Configurations classified as Type II under quasi-static loading produced sharp impulse peaks under impact, consistent with their high initial stiffness, while Type I configurations produced the lower, broader profiles corresponding to their progressive compliance.

This supports the expectation of Calladine and English [3] that a structure retains its characteristic response class under impact provided the impact velocity does not alter the quasi-static collapse mode, and extends that expectation to additively manufactured brittle architected cores, in which collapse proceeds by fracture rather than by plastic hinging. Quasi-static classification therefore has predictive value for the dynamic regime, at least at the incident energy examined here.

The practical implication, however, runs in the opposite direction to the intuition that static testing identifies the better impact performer. Because transmitted force tracks stiffness, the configuration that performs best under static loading is the one that performs worst as a protective element. Static screening on peak load will therefore systematically select against good attenuators, and protective performance must be assessed by direct measurement of transmitted force.

Table 2. Comparison of quasi-static compressive peak load with peak transmitted impact force for the same core configurations. Static values are reported in the companion study [9] and are reproduced here for comparison; the two quantities are measured under different conditions and are not directly equivalent.

Configuration	Static compression peak (N)	Impact transmitted (N)	Static class
Honeycomb 15°	1713.70 ± 446.45	1698.62 ± 200.29	Partial Type II
Honeycomb 30°	1778.61 ± 110.21	1741.61 ± 187.32	Type II
Honeycomb 45°	2283.27 ± 52.34	1926.47 ± 68.17	Type II
Honeycomb graded	2800.81 ± 82.41	1945.27 ± 43.44	Type II
Diamond 45°	8455.89 ± 138.33	2447.08 ± 42.38	Type II

© MAY 2023 | IRE Journals | Volume 6 Issue 11 | ISSN: 2456-8880
DOI: https://doi.org/10.64388/IREV6I11-1722650

Configuration	Static compression peak (N)	Impact transmitted (N)	Static class
Diamond 90°	2406.92 ± 164.84	1736.73 ± 295.31	Type II
Diamond 120°	408.19 ± 82.57	761.02 ± 27.30	Type I
Diamond graded	509.28 ± 70.65	775.35 ± 102.59	Type I

4.3 Attenuation is achieved by deformation, not fracture

The damage observations indicate that the configurations attenuating most effectively are those that fracture least. This is initially counterintuitive, since fracture consumes energy in the creation of new surface. The resolution is that in a brittle constituent, fracture is an inefficient dissipation mechanism per unit of core volume engaged: cracking releases stored elastic energy locally and does little to extend the duration of the contact event, so the impulse continues to be transmitted through the remaining intact load path. Large-scale compliant deformation, by contrast, engages a substantial fraction of the core volume and lengthens the contact interval, which directly reduces peak transmitted force.

For brittle architected cores intended for protection, this suggests that the design objective should be to promote distributed, bending-dominated core deformation rather than to maximise the energy consumed in fracture. A limitation follows directly: the permanence of the compliant deformation was not characterised in this study, so the extent to which these configurations would retain their attenuation capacity under subsequent impacts cannot be inferred from the present single-impact results.

4.4 Functional grading confines damage

The graded configurations demonstrated spatial control of damage rather than a simple change in magnitude. In the graded diamond core, fracture concentrated in the face sheet and upper row edges while the stiffer lower rows resisted deformation, and transmitted force remained close to that of the 120° configuration. In the graded honeycomb core, damage was confined within the central region and face sheet deflection was reduced relative to the 15° and 30° configurations.

In both cases the grading function, rather than the loading configuration, determined where damage was located. This permits damage to be directed away from regions that must retain integrity, such as load-introduction points or attachment features, and to be confined to a predetermined sacrificial zone. The graded honeycomb achieved this while transmitting a force comparable to the uniform honeycomb configurations, indicating that damage confinement did not require a penalty in transmitted force within this topology.

4.5 Limitations

Four limitations bound these results. First, the measured quantity is transmitted force at a sensor beneath the panel, not contact force at the impact point; the two are related through the panel response and should not be interchanged. Second, relative density was not held constant across configurations, since envelope and wall thickness were fixed while cell angle varied, so absolute values are not directly comparable across configurations of differing density and no specific-performance ranking is claimed. A density-controlled study is required for that purpose.

Third, a single incident energy of 5.4 J was applied, and the reported nominal velocity of 2.43 m/s neglects friction and drag within the guide tube. The static-to-dynamic correspondence reported in Section 4.2 is therefore established at one energy level and should not be extrapolated to velocities sufficient to alter the collapse mode. Fourth, the constituent was a brittle photopolymer selected to render fracture observable; ductile constituents would be expected to substitute plastic hinging for fracture in at least some configurations, and both the transmitted-force ranking and the damage extents may shift accordingly.

V. CONCLUSION

Low-velocity impact testing of eight two-dimensional architected sandwich core configurations, each subjected to a single impact at 5.4 J nominal incident energy, supports the following conclusions.

1. Peak transmitted force varied by a factor of 3.2 across the configuration set, from 2447.08 N for the 45° diamond core to 761.02 N for the 120° diamond core.
2. The honeycomb topology was insensitive to cell angle under impact, transmitting between 1698 and 1946 N across its full angular range, whereas the diamond topology spanned the entire measured range. Cell angle is therefore an effective design lever for impact attenuation in the diamond topology but not in the honeycomb topology.
3. Configurations transmitting the lowest force fractured least, dissipating incident energy through large-scale compliant core deformation rather than through cracking, and exhibited correspondingly broader force-time profiles. In brittle architected cores, attenuation is achieved by promoting distributed deformation rather than by maximising fracture.
4. The response classification established under quasi-static loading was preserved under impact, with Type II configurations producing sharp impulse peaks and Type I configurations producing lower, broader profiles, consistent with the framework of Calladine and English and extended here to brittle additively manufactured cores.
5. Because transmitted force tracks stiffness, the ranking by protective performance is inverted relative to the ranking by static strength. The stiffest configuration is the poorest attenuator, and static peak-load screening will systematically select against effective protective architectures.
6. Functional grading confined damage to prescribed core regions while leaving stiffer regions intact, with damage location determined by the grading function rather than by the loading configuration.

Future work should extend testing across a range of incident energies to establish the velocity at which the quasi-static correspondence breaks down, introduce relative-density constraints to permit equitable comparison across topologies, and assess multi-hit performance, which cannot be inferred from the single-impact results reported here.

REFERENCES

[1] M. F. Ashby and Y. J. M. Bréchet, "Designing hybrid materials," *Acta Materialia*, vol. 51, no. 19, pp. 5801–5821, 2003. ScienceDirect

[2] J. R. Greer and V. S. Deshpande, "Three-dimensional architected materials and structures: Design, fabrication, and mechanical behavior," *MRS Bulletin*, vol. 44, no. 10, pp. 750–757, 2019. Cambridge

[3] C. R. Calladine and R. W. English, "Strain-rate and inertia effects in the collapse of two types of energy-absorbing structure," *International Journal of Mechanical Sciences*, vol. 26, no. 11–12, pp. 689–701, 1984. ScienceDirect

[4] F. Zhu, G. Lu, D. Ruan, and Z. Wang, "Plastic Deformation, Failure and Energy Absorption of Sandwich Structures with Metallic Cellular Cores," *International Journal of Protective Structures*, vol. 1, no. 4, pp. 507–541, 2010. SAGE

[5] H. Yazdani Sarvestani, A. H. Akbarzadeh, A. Mirbolghasemi, and K. Hermenean, "3D printed meta-sandwich structures: Failure mechanism, energy absorption and multi-hit capability," *Materials & Design*, vol. 160, pp. 179–193, 2018. ScienceDirect

[6] S. Hou, T. Li, Z. Jia, and L. Wang, "Mechanical properties of sandwich composites with 3D-printed auxetic and non-auxetic lattice cores under low velocity impact," *Materials & Design*, vol. 160, pp. 1305–1321, 2018. ScienceDirect

[7] H. Niknam and A. H. Akbarzadeh, "Graded lattice structures: Simultaneous enhancement in stiffness and energy absorption," *Materials & Design*, vol. 196, p. 109129, 2020. ScienceDirect

[8] I. Maskery et al., "A mechanical property evaluation of graded density Al-Si10-Mg lattice structures manufactured by selective laser

melting," *Materials Science and Engineering A*, vol. 670, pp. 264–274, 2016. ScienceDirect

[9] B. Fadayomi, "Failure Modes and Fracture-Path Reproducibility in 2D Honeycomb and Diamond Sandwich Architected Cores Under Quasi-Static Loading," companion manuscript, submitted concurrently.